# A study on interlaminar behaviour of carbon/epoxy laminated curved beams by use of acoustic emission.

David Ranz[a,*], Jesús Cuartero[b], Luis Castejón[b], Ramón Miralbes[a]

[a] Design and Manufacturing Department, Zaragoza University, Zaragoza, Spain

[b] Mechanical Engineering Department, Zaragoza University, Zaragoza, Spain

## Abstract

The interlaminar tensile strength of carbon/epoxy laminated curved beams with variable thickness and through-the-thickness tufted reinforcement is studied experimentally by means of a four-point-bending test in accordance with ASTM D6415. These tests are monitored by means of the Acoustic Emission (AE) technique in order to gain deeper knowledge of the delamination onset and post-failure behavior. The results show that AE technique has proven to perform well when identifying delamination initiation and evolution after failure. In addition to this, AE has proven to be an appropriate tool to assess the manufacturing quality of the curved-beam, once a previous pattern has been established.

## Keyword

Interlaminar tensile strength, Delamination, Acoustic Emission, Laminated curved beam, Tufting.

## Introduction

Components of composite materials with high curve radii in their geometry are commonly present in a wide range of engineering structures found in fields as diverse as aviation, maritime, energy and civil engineering [1]. The main failure occurring in these components is due to interlaminar tensile stress, leading to delamination between layers [2, 3]. Therefore, determining the Interlaminar Tensile Strength (ILTS) and its subsequent evolution is key when approaching the development of efficient designs. As

* Corresponding author. David Ranz, Zaragoza University, C/ Maria de Luna 3, Edif. Torres Quevedo. Campus Rio Ebro, 50018-Zaragoza (SPAIN), Email: dranz@unizar.es

Ranz et al [4] show, there are several experimental methodologies available to determine ILTS. In the present study, an indirect load method – a four-point bending test on a curved test specimen in accordance with D6415 [5], is used.
The advantages and drawbacks of this methodology when compared with other direct and indirect methods, as well as its utilisation for the validation of ILTS values are found in different research studies [3, 6, 7, 8, 9]. In the present study, we assess – by establishing the Interlaminar Tensile Strength (ILTS) and its subsequent evolution – how the delamination onset/initiation is affected by of a range of lamination thicknesses and the inclusion of reinforcement through-the-thickness by means of tufting [10, 11, 12]. To that aim, an experimental study by means of mechanical tests monitored by means of Acoustic Emission (AE) in accordance with ASTM D6415 standard [5] is conducted. Those data results from mechanical test performed on specimens with different typologies, as well as their processing for getting ILTs and CBS, can be found at length in the research by Ranz [4].
The Acoustic Emission technique (AE) used for this study is a Non-destructive Testing (NDT) method based on the energy spontaneously released by a material when undergoing deformation. [13]. This elastic energy is released in materials under stress in areas where plastic deformation or crack growth take place.
Several authors [14, 15, 16, 17, 18] have utilised AE to predict damage and its evolution in composite materials, with the most common AE sources being: fibre rupture and tear, fibre pull-out, fibre/matrix debonding, matrix micro-cracking, matrix transverse failure, parallel detachment of fibres, and delamination. Most of these authors have determined that matrix cracking is linked to short duration events with low amplitude and low energy; fibre rupture is linked to short duration events with high amplitude; and delamination or interface failure of laminate composites is linked to long duration events, with a high number of counts and high amplitude and high energy.

## Experimental procedure

The test method used corresponds to ASTM D6415 standard [5], determining the Curved Beam Strength (CBS) of a composite material reinforced with continuous fibre, using a curved beam specimen (Figure *1*). ASTM D6415 standard establishes a standardised procedure in order to determine the ILTS for unidirectional fibre-reinforced composite test specimens.

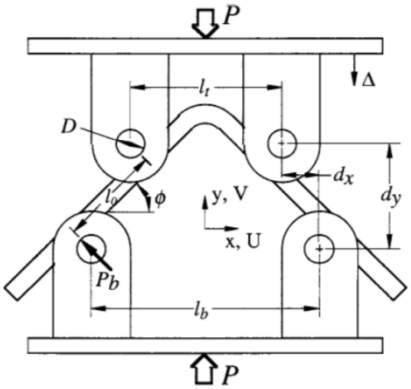


Figure 1. ASTM D6415 Test: Outline [5] (left); test specimen actual layout (right).

The curved test specimens were made of unidirectional carbon fabric (866 gr/m2) and a matrix system of epoxy resin, processed by means of the Liquid Resin Infusion method (LRI). By piling up 4, 8, and 12 layers, three different thicknesses were obtained, while the unidirectional carbon was oriented towards the test specimen´s legs and along the curved area [4]. In addition, and in order to improve the out-of-the-plane properties of the laminate, the stitching technique known as tufting was used [4]. For the reinforcement through the thickness, a continuous thread of glass fibre under the sales description EC9 68x3 S260 with a linear density of 1200 tex is used. For the three specimen thicknesses, two different tufting densities, D1 and D2 are used: for the first, glass fibre threads are separated at 10 mm intervals in both directions whereas, for the second, the separation is 5mm.

An 8032 INSTRON universal test machine with a load capacity of up to 100 KN is used, applying constant velocity 0.5mm/min.

AEWin acoustic emission software is used, as well as the 1283-USB-AE-Node by Physical Acoustics Corporation, with a 20 MHz maximum sampling frequency. An R15-Alpha piezoelectric sensor is used, with a resonance frequency of 151.37 kHz and an optimum operating range of 100-1000 kHz. The amplitude threshold was set at 40 dB for every test, a few dB above background noise.

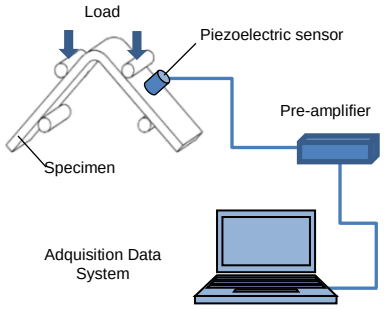


Figure 2. Description of the AE system.

# Test results from unidirectional test specimens, with and without tufting

## Bending test results on “curved beam” test specimens

*Figure 3* displays the load-displacement graphs for the tests where no stitching was involved and those tests where 2 different stitching densities for 4, 8 and 12 layer test specimens were used. In them, the differences in the load reached at failure as well as a high similarity in rigidity in the test specimens can be appreciated, regardless of the use of stitching. As for the post-failure behaviour of the test specimens, we can observe that, for those test specimens where stitching is absent, there is no recovery in their load capacity, whereas for those test specimens where stitching has been carried out, they retain their capacity under increased load, this effect being higher for those test specimens with higher stitching density (density 2). This capacity that the test specimen

has to retain its structural strength can be attributed to the stitching thread acting as an anchor between the different layers, thus preventing the rapid progression of delamination.

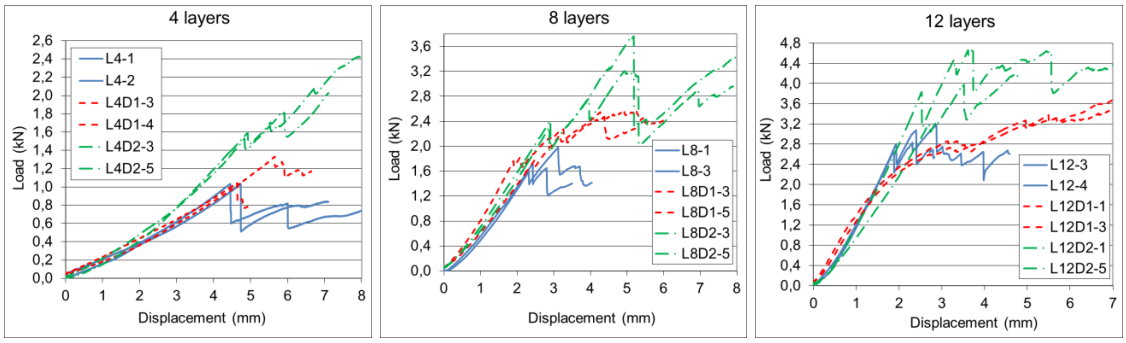


Figure 3. Load-displacement graphs for non-stitched test specimens, density 1 and density 2 for 4, 8 and 12 layers [4].

All graphs regarding test data results, as well as the majority of details on results and ILTS calculation can be found in a previous study [4]. As a summary, ILTS results and differences between different test specimen typologies can be found in *Table 1*. There, we can see that for both types of test specimens, i.e, those without stitching and those reinforced by using the tufting technique, the ILTS values decrease whenever there is an increase in thickness due to volumetric effects [3, 7, 1].

Table 1. Influence of tufting on ILTS for the different densities.

| | Non-Stitched | Density 1 | | Density 2 | |
|---|---|---|---|---|---|
| | ILTS (MPa) | ILTS (MPa) | Variation | ILTS (MPa) | Variation |
| 4 layers | **51,76** | **49,61** | -4,1% | **72,14** | 39,4% |
| 8 layers | **43,83** | **37,57** | -14,3% | **58,84** | 34,2% |
| 12 layers | **43,23** | **35,95** | -16,8% | **48,25** | 11,6% |

By and large, it is observed that test specimens tend to deform elastically until they reach a maximum load, resulting in a drop in the load, coinciding with the onset of delamination. This drop is rapidly checked, leading to a subsequent recovery in the test specimen´s load capacity, with gradients close to the initial ones, with small specific losses in load capacity, coinciding with delamination development. Nonetheless, it is worth pointing out that for Density 1, 12 layer curved test specimens, the load borne is even lower than those loads found in non-stitched test specimens. In addition, their bearing capacity after failure is much lower, with no further delamination taking place. This behaviour will be further analysed in section 3.3.

## AE results for non-stitched test specimens

Analysis of the AE parameters of tested specimens allows us to gain higher insights into failure, with information about the onset of failure in the composites, and its progression. Figure 4 and Figure 5 show the behaviour of the diverse events taking place during the loading process on non-stitched, 4 layer test specimens. There is an absence of acoustic events during the first loading stage (0 s to 260 s), which coincides with the area of elastic deformation. Nevertheless, once the maximum load has been reached, the first events of acoustic emission start to appear. After 260 seconds into testing time, a first delamination occurs, with a very high amplitude event (100 dB), high energy (14,700 attoJ) and a high number of counts, entailing a long duration event. As for the delamination occurring during the other interfaces (350 s and 500 s), we find events with very high amplitude, between 95 dB and 100 dB. Throughout the delamination propagation process of the different layers, the existence of lower amplitude events, within the 60 dB and 80 dB range, is ascertained. Once the delamination has started, there is an increase in the number of events and accumulated acoustic energy. This indicates continuous delamination propagation. The evolution shown in the graph for accumulated acoustic energy emitted coincides with the one representing the load throughout the testing time.

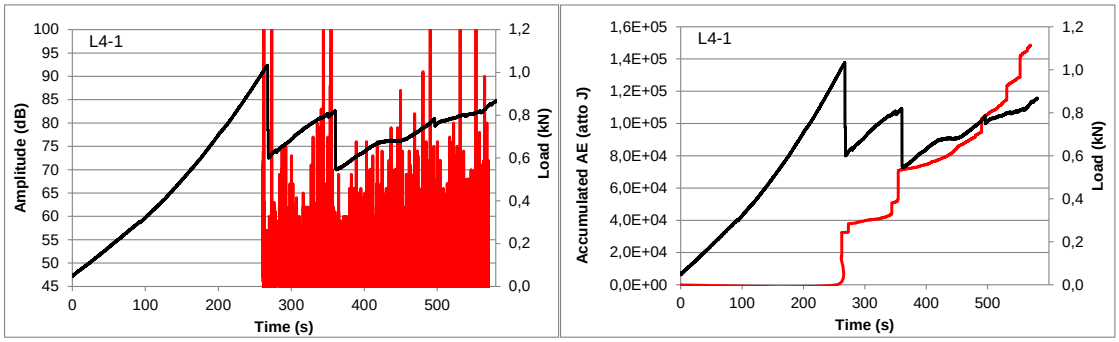


Figure 4. Load and accumulated acoustic energy for non-stitched, 4 layer test specimens.

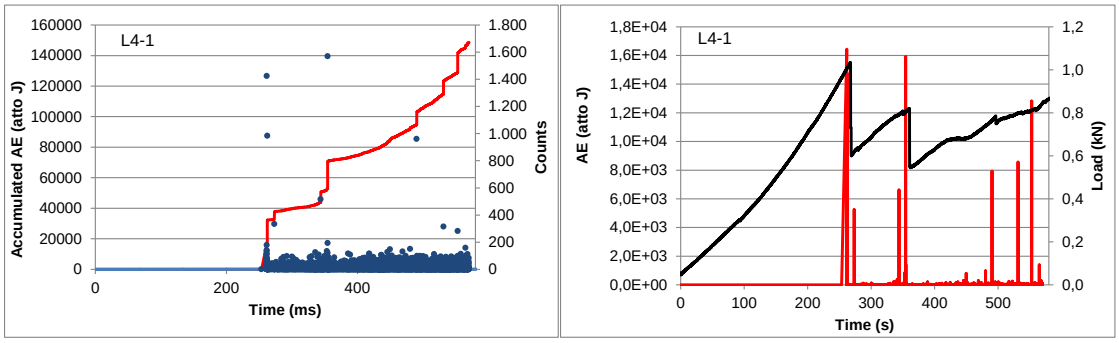


Figure 5. Counts and acoustic energy for non-stitched, 4 layer test specimens.

Figure 6 and Figure 7 show AE results for non-stitched, 12 layer test specimens. Whereas practically no acoustic events can be detected during the first stage of the loading process (0 s to 55 s), once a 2.65 kN load level has been reached, we find an event with high amplitude (98 dB) and energy (4,000 attoJ), coinciding with the first delamination. From

this moment onwards, several short duration, lower amplitude (60 dB to 80 dB) events continue to occur, which signposts a progression of the delamination front throughout the interface. This is so until the delamination of the next interfaces (70 s, 87 s, 105 s and 120 s) is reached, recognisable for being high amplitude (100 dB) events in the AE test, with high energy (over 7,000 attoJ) and a high number of counts (>500) coinciding with a significant drop in the load as shown in the force-time graph.

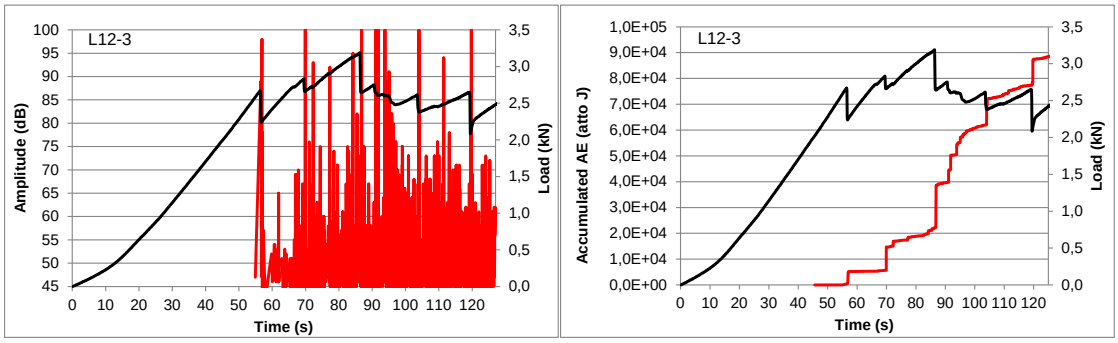


Figure 6. Load and accumulated acoustic energy for non-stitched, 12 layer test specimens.

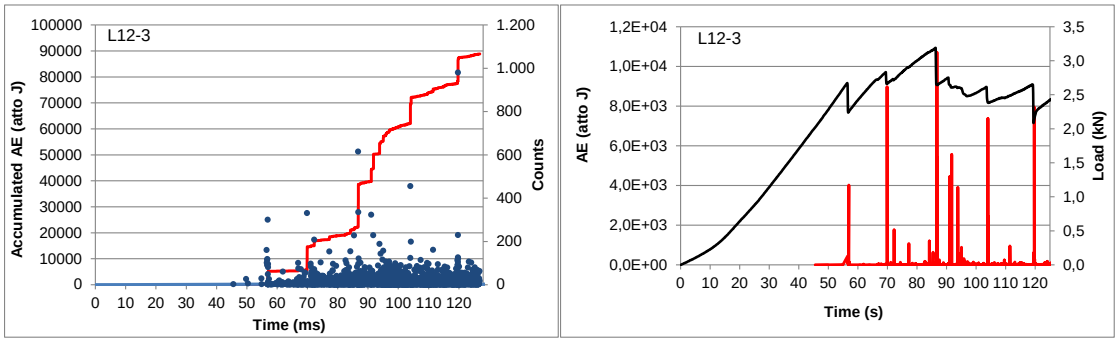


Figure 7. Counts and acoustic energy for non-stitched, 12 layer test specimens.

## Acoustic Emission results for test specimens reinforced by means of tufting

As in the previous section, the AE technique is similarly used in this one, to characterise the behaviour of 4, 8, and 12 layer UD test specimens reinforced through the thickness by means of two tufting densities. Figure 8 and Figure 9 show information for those events collected by the AE transductor on those stitched with D1 Density, 4 layer test specimens. In this instance, there is an absence of relevant events up to 170 seconds into testing time, when the first delamination happens, coinciding with a high amplitude (100 dB) and energy (9,000 attoJ) event. From that moment onwards, there are two very proximate instances of delamination (178 s and 198 s) with lower energy (2,000 attoJ and 5,000 attoJ) and, during the interval, we find further lower intensity events.

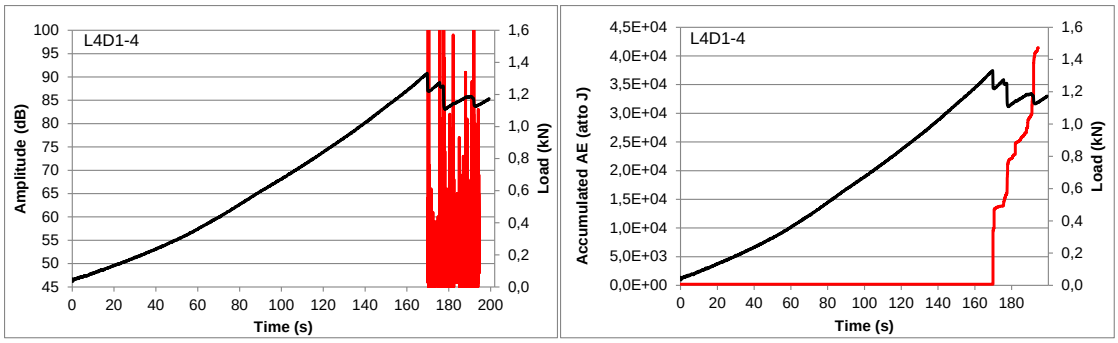


Figure 8. Load and accumulated acoustic energy for D1 stitching, 4 layer test specimens.

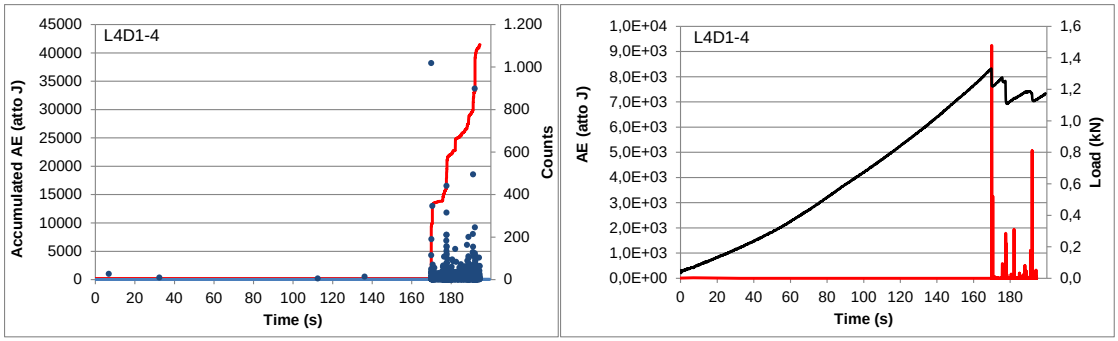


Figure 9. Counts and acoustic energy for D1 stitching, 4 layer test specimens.

For Density 1, 8 layer test specimens (Figure 10 and Figure 11), the first events occur after 58 seconds into testing time, coinciding with the first delamination. Furthermore, we can see subsequent instances of delamination ranging between 98 dB and 100 dB amplitude, and released acoustic energy ranging between 2,000 attoJ and 7,000 attoJ. The accumulated energy graph shows a parallel evolution with the force-time graph.

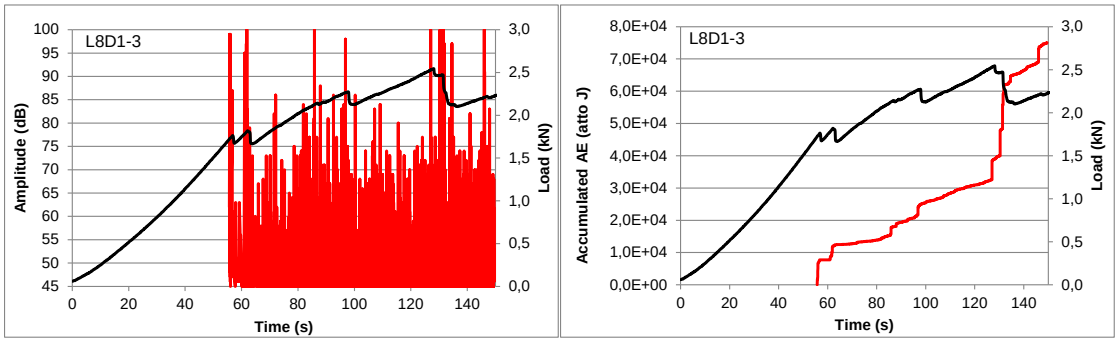


Figure 10. Load and accumulated acoustic energy for D1stitching, 8 layer test specimens.

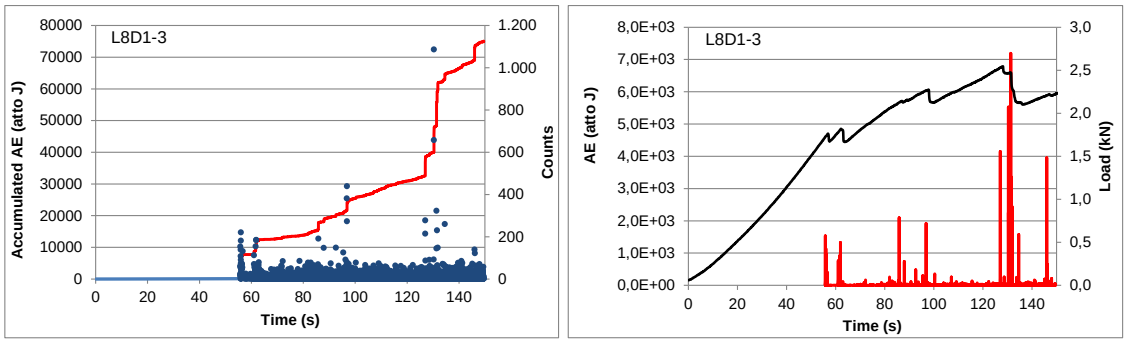


Figure 11. Counts and acoustic energy for D1 stitching, 8 layer test specimens.

When dealing with the Density 1, 12 layer test specimens (Figure 13 and Figure 14) we observe unique behaviour. As for the force-time graph, there is no sudden drop in the load and yet we do find early non-linearity in their elastic behaviour. Additionally, we observe acoustic events starting to happen at an early stage, from 20 s onwards, even prior to the reduction in the test specimens´ load bearing capacity.
A great number of low energy and short duration events take place during the loading process, leading to a high level of accumulated energy. Otherwise, there is good correlation between the accumulated energy and force-time curves.
Upon visual analysis of the test specimens in this batch (see Figure 12), still to undergo testing, the existence of layers with inadequate impregnation can be seen, leading to a loss in adhesion with adjacent layers, that is, there is induced delamination owing to some glitch during the manufacturing process.

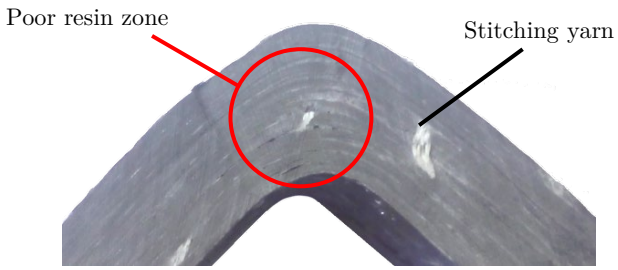


Figure 12. 12 layer test specimen with poor impregnation

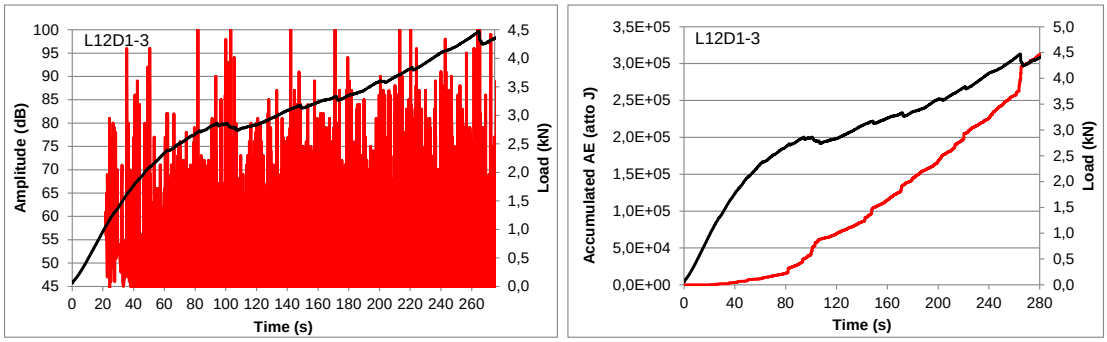

Figure 13. Load and accumulated acoustic energy for D1 stitching, 12 layer test specimens.

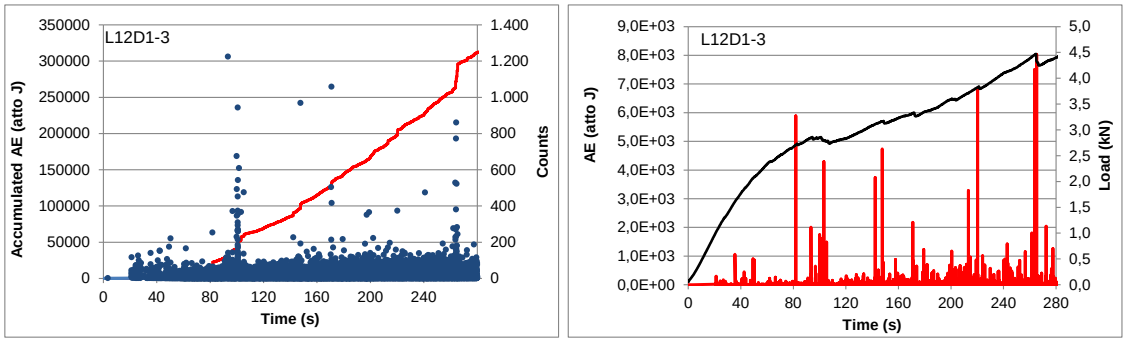


Figure 14. Counts and acoustic energy for D1 stitching, 12 layer test specimens.

Figure 15 and Figure 16 display information collected by the AE transductor on Density 2 stitching, 4 layer test specimens. In this instance, there is an absence of significant events up to 145 seconds into testing time, when the first delamination takes place, coinciding with a high amplitude (100 dB) and energy (8,000 attoJ) event. From that moment onwards, we find two very proximate instances of delamination (165 s and 200 s) with and energy of 8,000 attoJ and 5,500 attoJ, and during the interval, lower intensity events with amplitudes ranging from 60dB to 75 dB taking place, related to the delamination progress. While the released energy during the instances of delamination is high, no significant drop in the borne force can be observed in any of them.

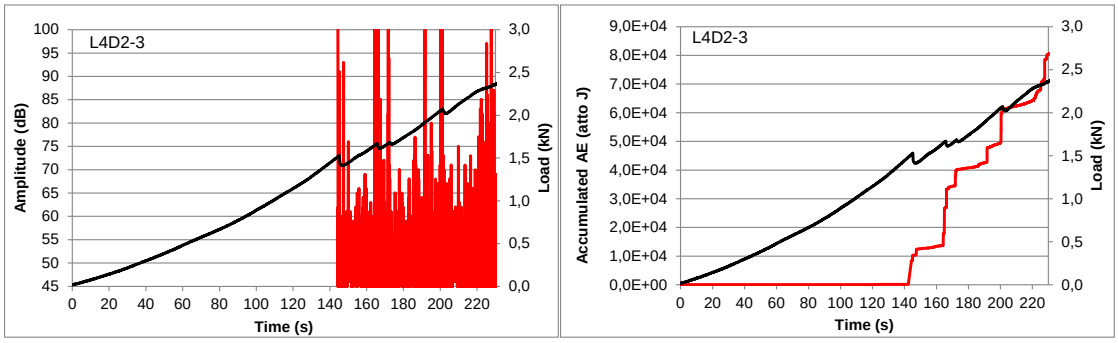


Figure 15. Load and accumulated acoustic energy for D2 stitching, 4 layer test specimens.

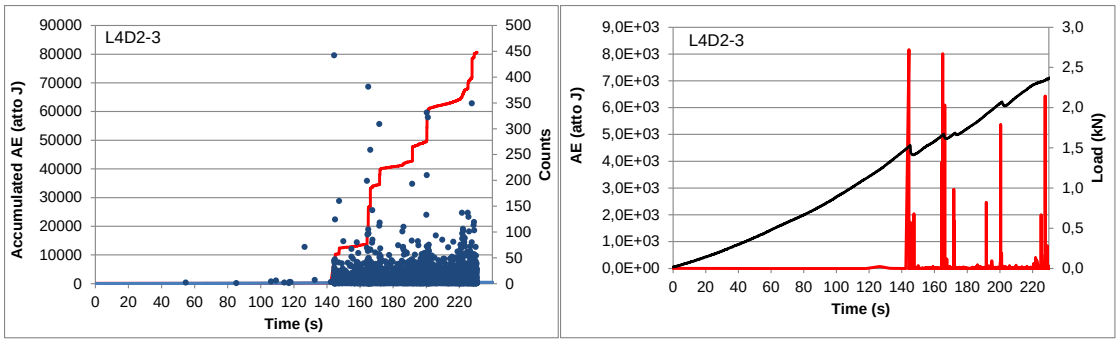


Figure 16. Counts and acoustic energy for D2 stitching, 4 layer test specimens.

AE data collected for Density 2, 8 layer test specimens (Figure 17 and Figure 18) shows that the first significant events occur after 87 seconds testing time, and coincide with the first delamination of 100 dB amplitude and released acoustic energy of 9,500 attoJ. Additionally, there are subsequent instances of delamination with amplitude close to 100 dB, at 120 seconds, 160 seconds and 210 seconds, with released acoustic energy of 13,000 attoJ, 40,000 attoJ and 10,000 attoJ, respectively. Throughout the interval between the instances of delamination, we find shorter duration events and low energy, ranging between 65 dB and 80 dB in amplitude.

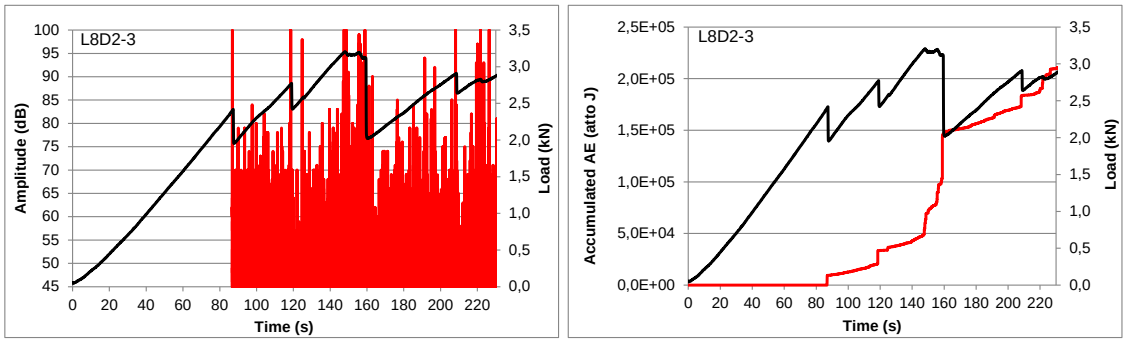


Figure 17. Load and accumulated acoustic energy for D2 stitching, 8 layer test specimens.

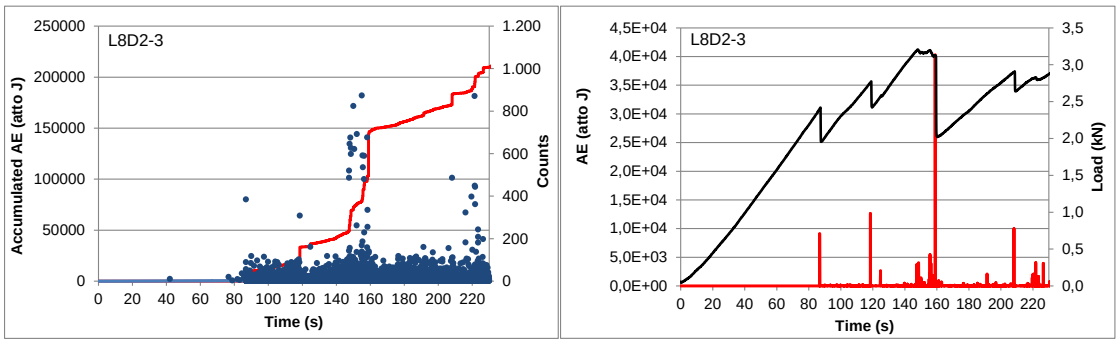


Figure 18. Counts and acoustic energy for D2 stitching, 8 layer test specimens.

Finally, for Density 2 stitching, 12 layer test specimens, (Figure 19 and Figure 20) we observe the same phenomenon as found in the previous cases: absence of acoustic events until the first delamination, which takes place at 80 seconds testing time. This first delamination occurs at high amplitude, with a high number of counts (300) and acoustic energy release of 4,000 attoJ. There are subsequent instances of delamination throughout the different interfaces, all of them with amplitude close to 100 dB and released acoustic energy from 7,500 attoJ to 12,000 attoJ.

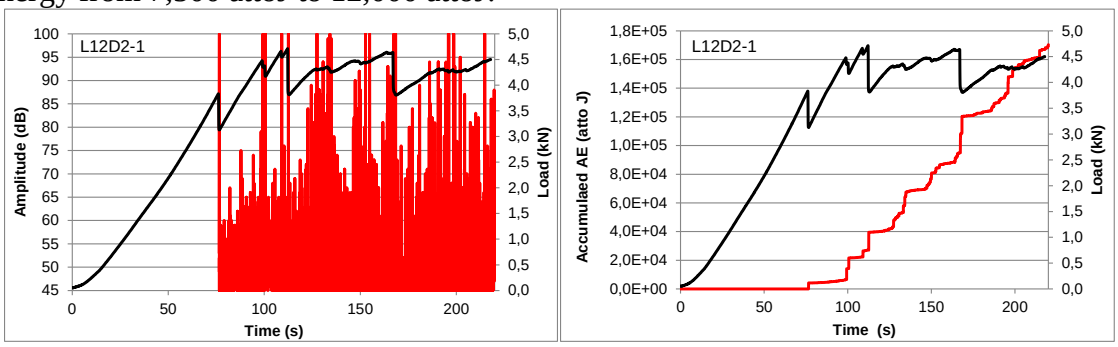


Figure 19. Load and accumulated acoustic energy for D2 stitching, 12 layer test pieces

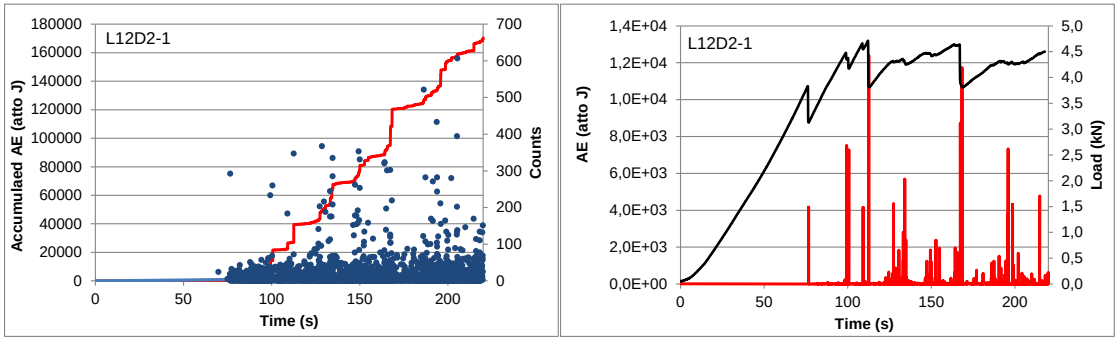


Figure 20. Counts and acoustic energy for D2 stitching, 12 layer test specimens.

# Conclusions

In all instances under study, it is observed that instances of delamination are detected since they generate high amplitude events – between 98 dB and 100 dB- and generate high acoustic energy release, normally ranging from 4,000 attoJ to 14,000 attoJ. This energy release is related to a drop in the load taking place. Thus, the higher the drop in the borne force, the higher the AE energy release collected. Throughout the interval when the diverse instances of delamination take place between the laminate interfaces, we find a large number of lower amplitude events, - from 60dB to 80 dB-, lower released energy (<1,000 attoJ) and shorter duration.

In all instances under analysis, it can be observed that the evolution of Acoustic Emission energy graphs show high correlation with data collected and displayed in the force-time graph. The main difference in the data collected in the Acoustic Emission tests between stitched and non-stitched test specimens is the lower number of low energy events taking

place in non-stitched test specimens, as well as lower values for accumulated acoustic emission energy (see *Figure 21*).

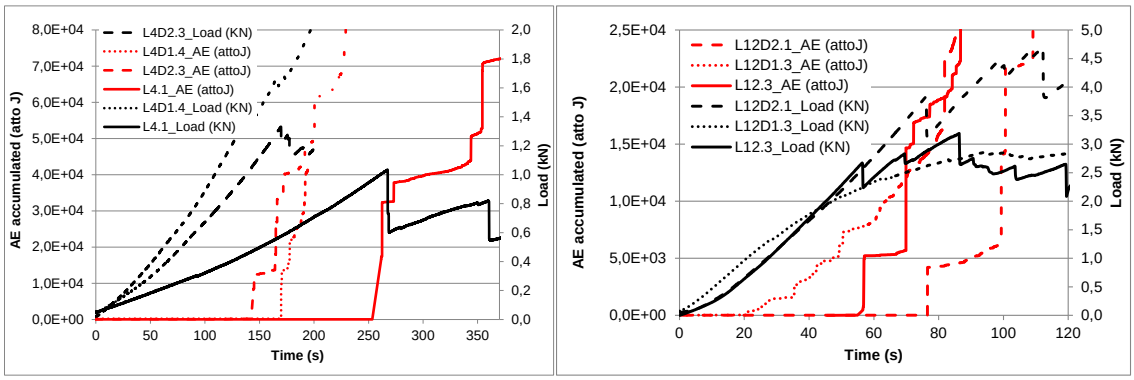


Figure 21. AE comparison for stitched & non-stitched test specimens:
(left) 4 layers; (right) 12 layers

Acoustic emission tests not only provide us with insights into test specimen failure characterisation, but also can be utilised as a tool to evaluate the quality of those test pieces manufactured, and by extension, of components manufactured from composites, provided that behavioural patterns based on orientation and piling-up are available. The usefulness of making use of this tool for quality assessment is evident in the instance of D1 stitching, 12 layer test specimens, where manufacturing glitches leading to differentiated AE behaviour were detected.

## Funding

The author(s) received no financial support for the research, authorship, and/or publication of this article.

## References

[1] W. Hao, D. Ge, Y. Ma, X. Yao and Y. Shi, «Experimental investigation on deformation and strength of carbon/epoxy laminated curved beams,» *Polymer Testing*, vol. 31, nº 4, p. 520–526, 2012.

[2] D. Raju, «Delamination damage analysis of curved composites subjected to compressive load using cohesive zone modelling,» *QuEST Global*, 2014.

[3] W. Cui, L. Jianxin and R. Ruo, «Interlaminar tensile strength (ILTS) measurement of woven glass/polyester laminates using four-point curved beam specimen,» *Composites Part A*, vol. 27A, pp. 1097-1105 , 1996.

[4] D. Ranz, J. Cuartero, A. Miravete and R. Miralbes, «Experimental research into interlaminar tensile strength of carbon/epoxy laminated curved beams,» *Composites Structures*, vol. 164, pp. 189-197, 2017.

[5] «ASTM D6415/D6415M-06a − Standard Test Method for Measuring the Curved Beam Strength of a Fiber-Reinforced Polymer-Matrix Composite,» West Conshohocken, PA, 1999.

[6] W. Jackson and P. Ifju, «Through the thickness tensile stress of textile composites,» NASA. Langley Research Center, 1994.

[7] W. Jackson and R. Martin, «An interlaminar tensile strength specimen,» *Composite Materials: Testing and Design*, vol. 11, pp. 333-354, 1993.

[8] E. Hara, T. Yokozeki and H. Hatta, «Comparison of out-of-plane tensile strengths of aligned CFRP obtained by 3-point bending and direct loading tests,» *Composites: Part A*, nº 43 , p. 1828–1836, 2012.

[9] A. Vänttinen, «Strength Prediction of Composite Rib Foot Corner,» Master's Thesis, Helsinki University of Technology, 2008.

[10] M. Colin de Verdiere, «Effect of Tufting on the Response of Non Crimp Fabrics Composites,» de *ECCOMAS Thematic Conference on Mechanical Response of*

*Composites*, Porto, Portugal, 2007.

[11] G. Dell'Anno and others, «Exploring mechanical property balance in tufted carbonfabric/epoxy composites,» *Composites: Part A*, vol. 38, p. 2366–2373, 2007.

[12] G. Dell'Anno, J. Treiber y I. Partridge, «Manufacturing ofcompositepartsreinforcedthrough-thickness by tufting,» *Robotics and Computer-Integrated Manufacturing*, 2015.

[13] R. Miller and P. McIntire, «Acoustic emission testing. American Society for Nondestructive Testing,» *Nondestructive testing handbook*, vol. 5, nº 2, p. 603, 1987.

[14] C. Ageorges, K. Friedrich, T. Schuller and B. Lauke, «Single-fibre Broutman test: fibre-matrix interface transverse debonding.,» *Composites: Part A*, vol. 30, p. 1423–1434, 1999.

[15] S. Huguet, N. Godin, R. Gaertner, L. Salmon and D. Villard, «Use of acoustic emission to identify damage modes in glass fibre reinforced polyester,» *Composite Science and Technology*, vol. 62, p. 1433–1444, 2002.

[16] P. Liu, J. Chu, Y. Liu and J. Zheng, «A study on the failure mechanisms of carbon fiber/epoxy composite laminates using acoustic emission,» *Materials and Design*, vol. 37, p. 228–235, 2012.

[17] M. Saeedifar, M. Fotouhi, M. Najafabadi and H. Toudeshky, «Prediction of

delamination growth in laminated composites using acoustic emission and Cohesive Zone Modeling techniques,» *Composite Structures,* vol. 124, pp. 120-127, 2015.

[18] L. Li, S. Lomov, X. Yan and V. Carvelli, «Cluster analysis of acoustic emission signals for 2D and 3D woven glass/epoxy composites.,» Composites Structures, vol. 116, p. 286–99., 2014.